

COLLAGEN ORIENTATION AND MOLECULAR SPACING DURING CREEP AND STRESS-RELAXATION IN SOFT CONNECTIVE TISSUES

PETER P. PURSLOW^{1,*}, TIM J. WESS² AND DAVID W. L. HUKINS³

¹*School of Molecular and Medical Biosciences, University of Wales College of Cardiff, UK*, ²*Department of Molecular and Biological Sciences, University of Stirling, UK* and ³*Department of Bio-Medical Physics and Bio-Engineering, University of Aberdeen, UK*

*Present address: Department of Dairy and Food Science, The Royal Veterinary and Agricultural University, Rolighedsvej 30, DK-1958 Frederiksberg C, Copenhagen, Denmark (e-mail: ppp@kvl.dk)

Accepted 6 October 1997; published on WWW 9 December 1997

Summary

Collagen fibres form cross-helical, cross-ply or quasi-random feltworks in extensible connective tissues; strain-induced reorientation of these networks gives rise to the non-linear mechanical properties of connective tissue at finite strains. Such tissues are also generally viscoelastic (i.e. display time-dependent properties). The hypothesis that time-dependent reorientation of collagen fibres is responsible for the viscoelasticity of such tissues is examined here using time-resolved X-ray diffraction measurements during stress-relaxation and creep transients applied to rat skin and bovine intramuscular connective tissue. Differences in the intensity and angular orientation of the third and fifth orders of the 67 nm meridional D-spacing of collagen

molecules were shown before and after the application of loads or displacements. However, no changes in the D-spacing or angular orientation of collagen occurred during the time course of either stress-relaxation or creep in both tissues. This indicates that collagen fibre reorientation is not a primary source of their viscoelastic properties. The non-linear (strain-dependent) nature of the stress-relaxation response in these tissues suggests that relaxation processes within the collagen fibres or at the fibre–matrix interface may be responsible for their viscoelastic nature.

Key words: mechanical properties, muscle, skin, synchrotron radiation, viscoelasticity, X-ray diffraction, connective tissue.

Introduction

Extensible connective tissues (e.g. skin, blood vessels, fascia) contain networks of fibrous collagen in an amorphous matrix. It is the reorientation of the collagen fibres within these networks that allows large extensions of the tissues and is responsible for their non-linear stress–strain curves (Wainwright *et al.* 1976). In some connective tissues (CTs), such as skin or artery wall, the collagen forms almost random feltworks (Bigi *et al.* 1981). In others, such as the perimysial connective tissue separating muscle fascicles (Purslow, 1989), the wall of the intestine (Gabella, 1987) and the annuli of the intervertebral disc (IVD) (Klein and Hukins, 1982), there is a crossed-ply or crossed-helical arrangement of fibres with respect to the long axis of the tube (gut), muscle fibre direction (perimysium) or cranio-caudal axis (IVD).

The long-range extensibility of tissues such as skin, perimysium and gut wall is accommodated by significant reorientation of their collagen fibre networks (Gabella, 1987; Rowe, 1974; Purslow, 1989). These extensible CTs also become progressively stiffer as they are extended and the collagen fibres become more aligned with the direction of stretching. This non-linear mechanical behaviour has been quantitatively related to the effects of strain-induced reorientation on the stiffness of collagen networks in blood vessels (Roveri *et al.* 1980; Bigi *et al.* 1981),

IVD (Klein and Hukins, 1982) and intramuscular CT (Purslow, 1989; Purslow and Trotter, 1994). A theoretical formulation for strain-induced reorientation has been presented (Aspden, 1986).

As with many other biological materials, extensible CTs are also viscoelastic, i.e. their mechanical properties are time/frequency dependent (Fung, 1980; Wainwright *et al.* 1976; Dorrington, 1980). This can be demonstrated by the application of a fixed extension to the tissue, with the result that the initial stress generated decreases with time (stress-relaxation), or by the application of a fixed stress, whereupon the initial extension in the tissue increases with time (creep). Time-dependent effects are important in the functioning of some CTs, as they can serve in damping transient stresses. Viscoelastic behaviour in intramuscular CT is interesting as it implies that the CT structures could contribute to the modulation of the mechanical outputs of the contractile elements of muscle.

It is a common assumption that the time-dependent reorientation of collagen fibres within a viscous matrix explains the viscoelastic behaviour of extensible CTs (Wainwright *et al.* 1976), although this hypothesis does not seem to have been tested experimentally. An alternative hypothesis could be that viscoelastic effects arise from molecular relaxations within the proteoglycan matrix surrounding the collagen fibres or within

the collagen fibres themselves. In tendons, where collagen fibres are aligned with the long axis of the tissue, viscoelastic behaviour at small strains (approximately 5% longitudinal strain) has been interpreted on the basis of extension of the quarter-stagger overlap (D-periodicity) between molecules (Mosler *et al.* 1985). The hypothesis that reorientation of collagen fibres is not time-dependent is consistent with the response of IVD to compression, torsion and bending (Klein and Hukins, 1982). The actual mechanisms responsible for time-dependent aspects of the mechanical properties of extensible CTs are, therefore, undetermined, and the findings of Klein and Hukins (1982) provide some circumstantial evidence to doubt the commonly assumed explanation.

The present paper describes experiments designed to test in outline whether the time course of transient mechanical responses to step-extension or loads seen in extensible CTs is matched by the time course of reorientation in their collagen network. Time-resolved X-ray diffraction is used in this context as a means to measure any changes in collagen fibre orientation and also to measure any changes in the molecular packing within collagen fibres. Experiments were conducted on two connective tissues; rat skin and bovine perimysium. The perimysium is used because it is a uniform thin sheet of connective tissue with a well-organised crossed-ply collagen fibre arrangement and because collagen fibre orientation has previously been measured in perimysium and related to its static elastic properties (Purslow, 1989). Rat skin is used as an archetypal example of a connective tissue composed of a pseudo-random collagen fibre network.

Materials and methods

Principles of the X-ray technique used to measure molecular spacing and the orientation of collagen

X-ray diffraction of biological tissues rich in collagen produces diffraction images that contain a number of features due to the interaction of X-rays with molecular spacings within the tissue. In connective tissues, the fibrillar collagen structures produce the predominant interaction. Within the collagen fibril is a highly ordered axial arrangement of molecules where nearest neighbours are staggered by 67 nm (the quarter-stagger model). This generates a repeating periodic function 67 nm long that acts as a molecular diffraction grating. The resulting X-ray diffraction pattern is dominated by Bragg reflections that correspond to the 67 nm spacing and harmonic frequencies of this spacing (67/2 nm, 67/3 nm ... 67/n nm where n is an integer). The reflection for the fundamental 67 nm spacing is referred to as the first-order reflection, that from 67/2 nm as the second order, that from 67/3 nm as the third order, etc. The diffraction maxima arise from axial (longitudinal) spacings along the fibrils and are therefore aligned along the longitudinal direction in the X-ray pattern (known as the meridional direction in the pattern). This is shown schematically in Fig. 1A. Any effect that alters the fundamental periodicity of the structure would also alter the meridional position of the Bragg reflections on the detector.

In single X-ray crystallography, the crystal of a biological macromolecule is highly ordered in three dimensions, producing

relatively sharp diffraction spots; in order to collect a whole data set of Bragg intensities, the crystal must be rotated so that all available spacings are at some stage correctly orientated to the beam in order for diffraction to occur. This is different from the diffraction of natural, fibrous biological tissues. In a tissue such as skin, collagen fibrils have an axial arrangement that is more ordered than the lateral association; therefore, the axial meridional reflections are predominant in the observed diffraction pattern. In most membranous connective tissues, the orientation of fibrils in or near the plane of the tissue means that fibril orientations are suitable for strong diffraction from a beam passing through the thickness of the tissue. The relative orientation of fibrils in the plane of the tissue causes the Bragg reflections from individual fibrils to appear at different positions on an arc or circle corresponding to a given molecular spacing (Fig. 1B). Since the structure contains a large number of fibrils, the distribution of intensity around an arc is smooth. Variations in intensity of the reflections with angular position therefore reflect the distribution of angular positions in the population of collagen fibrils sampled by the beam. If the fibrils are orientated completely randomly, a uniform circle of isotropic diffracted intensity is obtained at a distance corresponding to one molecular spacing. If preferentially orientated, the diffracted intensity forms strong arcs centred on the orientation direction. Transforming the pattern from Cartesian (x, y) coordinates to polar (r, θ) coordinates facilitates its interpretation and quantitation (Fig. 1C). In polar coordinates, a reflection in the original Cartesian X-ray pattern which lies along an arc of a circle now lies along a straight line, at constant radius r . The length of the line represents the angular span (θ). For a random array of fibrils (producing a uniform, circular Cartesian diffraction pattern), a polar plot of the data produces a straight line of uniform intensity with respect to θ . If the fibrils are preferentially orientated (e.g. by straining the tissue), then a plot of intensity *versus* θ yields a peak centred on the preferred orientation direction. The width at half-maximum intensity of such an intensity distribution has previously been used to describe the degree of orientation of a collagen fibril population (Roveri *et al.* 1980).

Experimental protocol

The skin between the pelvic and pectoral girdles of female Wistar rats (approximately 8 weeks old) was shaved and removed immediately *post-mortem*, moistened with saline and frozen until use at -20°C . Strips of skin approximately 3–5 mm wide were then cut, with the long direction of the strips parallel to the original transverse axis of the animal. The semitendinosus muscle from a Friesian-cross heifer approximately 18 months old was excised *post-mortem*, sliced into 1 cm thick transverse sections and frozen at -20°C until use. Samples of the perimysial connective tissue that separates muscle fascicles were then carefully dissected from thawed muscle slices under a stereomicroscope (CZ JENA Technival 2, Germany) and cut into strips (approximately 3–5 mm wide), with the long direction of the strip parallel to the circumferential axis of the muscle fascicle.

Strips of skin and perimysium were glued with cyanoacrylate (LOCTITE, UK) to templates of thick

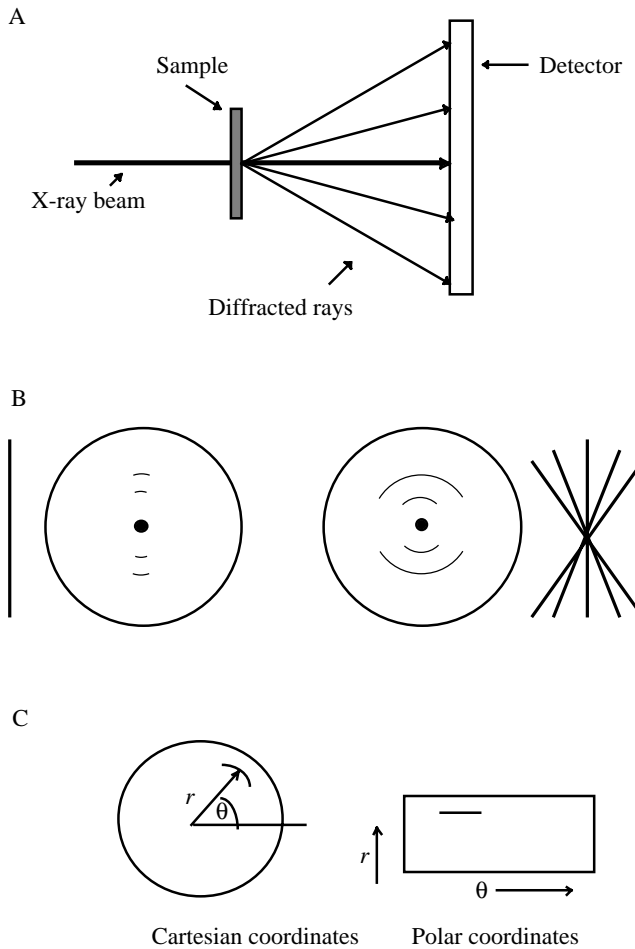


Fig. 1. Schematic diagram of the basis of the X-ray diffraction technique. (A) Side view of the diffraction of X-rays from a specimen. Much of the main beam is undiffracted and passes straight on to the detector. The rays drawn from the specimen to the detector (other than the main beam) represent just two orders of the diffraction from an axial spacing d in the specimen. These diffraction maxima occur at angles 2θ to the main beam, where $\sin\theta = \lambda n/2d$ (Bragg reflections). λ is the wavelength of the X-rays used, and n is the order of the reflection (e.g. $n=1$ and 2 in this schematic example). This condition is satisfied for angles θ in both the upper direction and the lower direction, so that a pattern symmetrical about the horizontal axis is produced. Note that θ and d are reciprocally related; with suitable calibration, values of $1/d$ (reciprocal space) can be read off the detector (see Figs 5 and 6). (B) Plan views of the detector, showing (left) the alignment between the position of the two orders of reflections and the axial direction of a single collagen fibre and (right) the angular spreading of these reflections due to angular dispersions of a population of collagen fibres. (C) Conversion of a pattern containing a reflection lying on a circular arc from Cartesian (x,y) to polar (r,θ) coordinates results in a straight-line representation of the reflection. Intensity can be measured along this line and plotted against angular position.

aluminium foil such that the long axis of the strip ran across a 14 mm long rectangular window cut in the template. The mounting of specimens on templates ensured that undue stretching of samples during subsequent mounting in the apparatus was avoided.

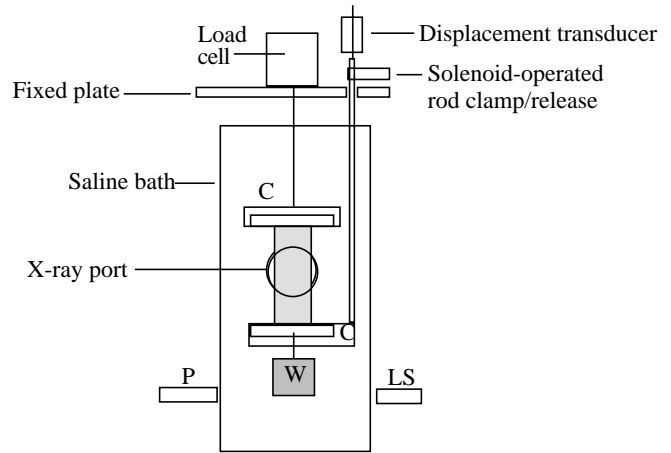


Fig. 2. Diagram of the mechanical transient apparatus. C, clamp plates; P, photodiode; LS, light source; W, drop weight. For stress-relaxation experiments, step displacements were applied by allowing the rod holding the bottom clamp to drop by pre-set amounts, *via* the solenoid release; displacement was monitored *via* the transducer attached to the rod. For creep experiments, the lower clamp was not glued to the bottom tab holding the specimen, but merely supported it. On release of the solenoid, the rod and the lower clamp then dropped away completely, allowing the drop weight W to load the specimen. The time-dependent displacement in the specimen was monitored by detecting the position of the weight *via* its interception of the light from source as detected by the photodiode. Two X-ray ports (Mylar windows) immediately in front of and behind the specimen allowed X-ray irradiation of the specimen during these mechanical transients.

Template-mounted specimens were glued with cyanoacrylate to the clamp plates of the apparatus shown in Fig. 2, which was designed to apply known rapid displacements and to record loads over time (stress-relaxation test) or rapidly to apply known loads and to monitor displacements over time (creep) test. Immediately prior to the test, the sides of the aluminium template were carefully cut away, leaving the specimen as the only structure bridging the space between the clamp plates. The specimen during these mechanical tests was immersed in 0.9% NaCl in a bath with Mylar windows to allow the passage of X-rays. The windows were on the ends of adjustable telescopic tubes that projected into the bath, such that the two inlet and outlet windows could be positioned very close to the surface of the specimen, thus minimising the length of the X-ray path through the saline to approximately 1–2 mm. The whole apparatus was mounted in the X-ray beam line of station 2.1 at the Daresbury Laboratory Synchrotron Radiation Source. A fast two-dimensional area detector constructed by the Daresbury Laboratory detector group (Hall and Lewis, 1994) was used to record diffraction patterns from the specimen, using an evacuated camera length of 3.25 m. The monochromatic beam of wavelength 1.488 nm was focused at the detector with a beam size of 1 mm in height and 2 mm in width. Detector response measurements were made to correct for the positional variations in the efficiency of the detector and for positional non-linearities. Empty specimen cell measurements were also made for the appropriate time frames.

Creep or stress-relaxation transients were applied to the specimens ($N > 10$) for periods ranging from 90 to 1500 s (25 min), and load and displacement signals were monitored throughout. X-ray diffraction patterns were obtained immediately prior to the mechanical transient and at intervals during the duration of the transient, with near-exponentially increasing time intervals between each exposure. The time course of these series of exposure frames is indicated in Fig. 3. On short transients (90 s), all exposure times were 2 s, and 11 separate patterns (1 pre-transient + 10 during the transient) were taken. On long transients (25 min), 11 patterns were again taken at increasing intervals and with 2 s exposures before and immediately after application of the transient, but with 10 s exposures thereafter. Each series of diffraction images was digitally captured using the Daresbury Laboratory NCD acquisition software and subsequently analysed using either the Daresbury BSL software or image analysis routines written specifically for this analysis. The design of the apparatus (Fig. 2) allowed progressive lengthening steps to be applied in a succession of stress-relaxation tests on a given specimen. A time series of diffraction images could therefore be captured in stress-relaxation on stretching the tissue by fixed amounts from a controlled range of pre-strains.

Analysis of X-ray patterns

The angular distribution and radial position of reflections corresponding to the third and fifth orders of the 67 nm meridional spacing from collagen molecules were analysed by converting the detector images to a polar coordinate system. This required the centre of the diffraction image to be determined for each creep or stress-relaxation series. The centre was easily located by the use of a semi-transparent beamstop that allowed the main beam to be imaged on the detector.

The use of the centre-finding routines in the FIT2D software written by A. Hammersley of ESRF (Hammersley, 1993) confirmed the suitability of this approach. In conversion to polar coordinates, each pixel point was re-mapped onto a point in polar space, and the grid was then re-mapped to produce a 512×512 image where the ordinate corresponds to the reciprocal (radial) spacing r and the abscissa corresponds to the function of angular distribution (θ). From these maps, it is a simple procedure to examine integrations along lines parallel to the r or θ directions. (For example, integration over a small range of r was made to measure the total intensity in a reflection as a function of θ ; similarly, integrations over a range of values of θ were performed to produce plots of total intensity *versus* radial position for a given reflection.) The same integrations could be readily made for a series of time frames, and the exposure time of each normalised. For a typical sample, the beam intensity increased by 7% after the initial stretch but thereafter showed less than 2% variation (coefficient of variation), with no apparent pattern. It is therefore assumed that the beam flux was stable during each series of diffraction events and that changes in intensity were due to changes in the sample characteristics. The plots of intensity *versus* radial position could be smoothed using a median function with a typical size of 9 pixel points and then output as a series of overlaid peaks. The diffraction pattern exhibits significant low-

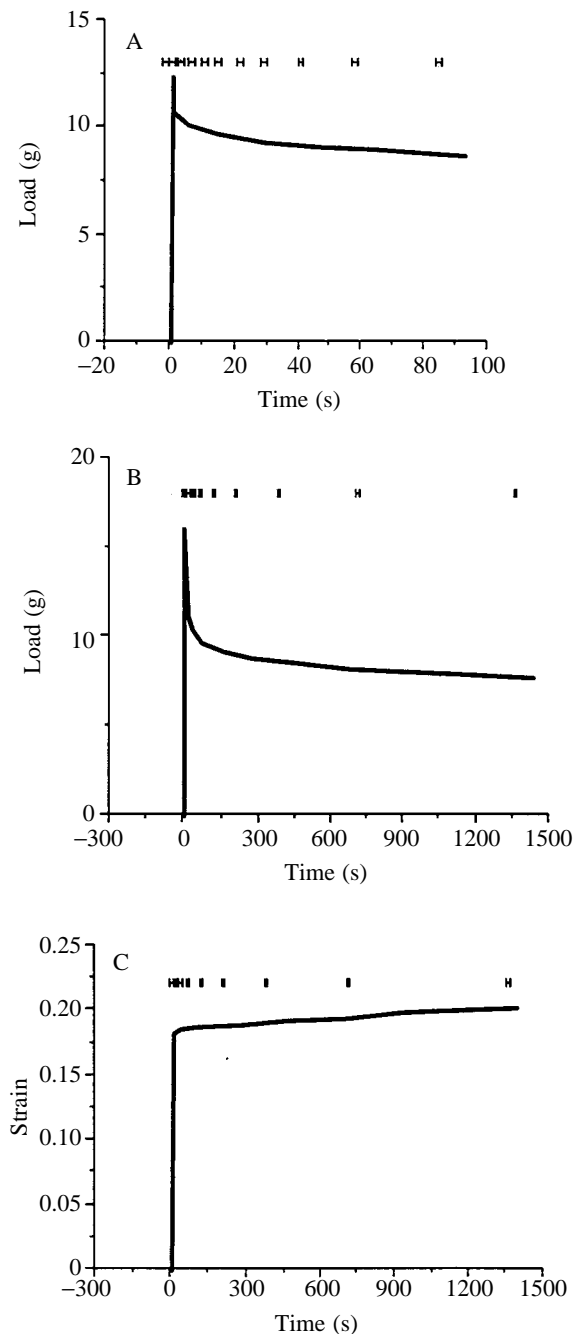


Fig. 3. Typical stress-relaxation curves for (A) perimysium and (B) rat skin and (C) a creep curve for rat skin. Note the change in time scale between A and B. Bars above each trace show the time and duration of 11 frames of X-ray diffraction information collected in each experiment. In C, the applied stress was 0.028 MPa.

angle scatter from the sample along the equator; this shows as a peak oriented at 90° from the meridional diffraction.

Results

Fig. 3 shows typical stress-relaxation behaviour for perimysium (Fig. 3A) and rat skin (Fig. 3B) and the creep behaviour of rat skin (Fig. 3C). The small bars across the top

of the figures indicate the time frames for X-ray diffraction pattern collection in each case. Fig. 4 shows a polar (r, θ) plot of a typical diffraction pattern obtained from the middle of the creep transient shown as Fig. 3C. Because the pattern is symmetrical, it is only necessary to analyse one half of the pattern ($\theta=0-180^\circ$). The third and fifth orders of the 67 nm meridional spacing are clearly visible in this pattern.

Fig. 5 shows the results from an analysis of the X-ray diffraction patterns taken during the time course of the stress-relaxation test on rat skin shown as Fig. 3B. In Fig. 5A, the intensity of diffracted X-rays *versus* radial position r is shown for all 11 time frames (1 pre-transient + 10 during mechanical transient). The peaks marked third and fifth order correspond to the third and fifth order of the 67 nm meridional D-spacing of collagen. The intensity of patterns taken during the transient was greater than that of the pre-transient pattern (marked 1). This may possibly be due to alignment of out-of-plane collagen fibres, to concentration of collagen in a thinner (stretched) specimen or to higher loads/extensions improving the regularity of the meridional spacings. No differences in the radial position of the intensity maxima were observed, indicating that there was no measurable increase in D-spacing during the course of the

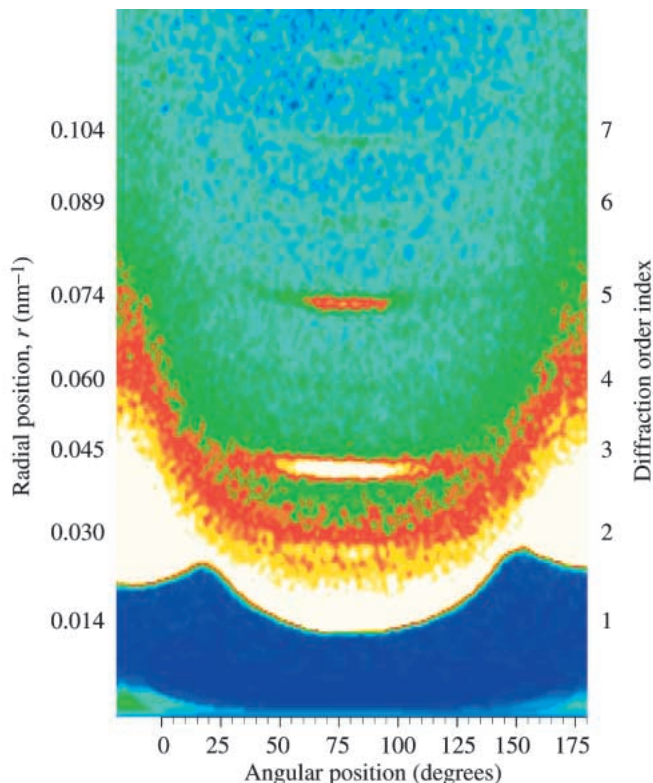


Fig. 4. Typical X-ray diffraction data collected from rat skin plotted on polar (r, θ) coordinates. For clear identification of diffraction maxima, this colour representation shows X-ray intensity increasing in the colour order: blue, green, red, yellow, white. One of the two sets of diffraction maxima due to orders of the 67 nm meridional spacing in collagen is shown; the other set is disposed at 180° to this set. The numbers on the right-hand side indicate the expected position for the n th order reflections ($n=1, 2, 3, \dots$) from the 67 nm axial D-spacing of collagen.

experiment. (Neither could a change in D-spacing be seen at the maxima corresponding to the ninth and twelfth orders, where any small spacing changes should be more easily discerned because a small percentage change in the spacing would translate into a proportionately larger absolute change in the maxima on the

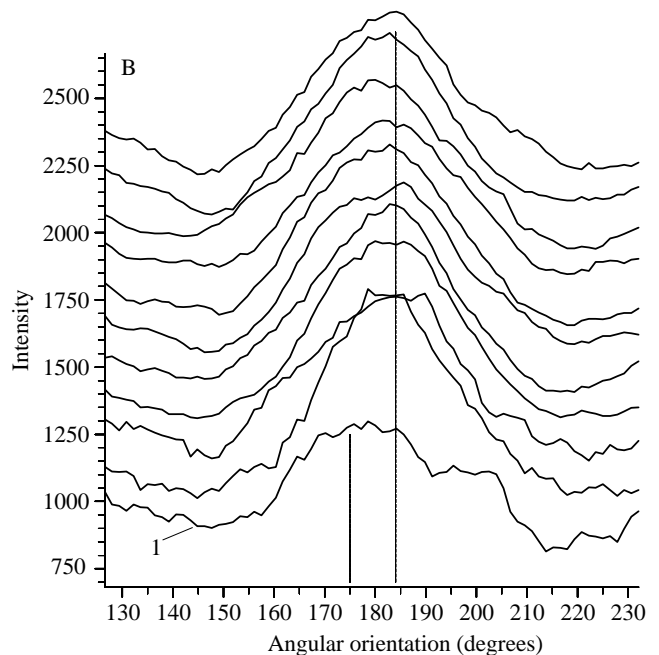
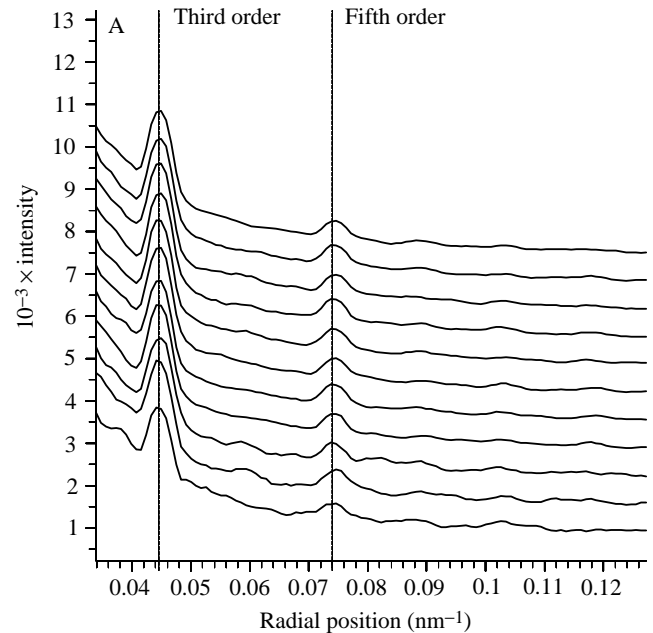


Fig. 5. Meridional spacing and angular distribution of intensity maxima during stress-relaxation in rat skin. (A) Intensity *versus* radial position on the detector, corresponding to $1/d$ (nm). The dotted lines indicate the positions of the third and fifth orders of the collagen D-spacing. (B) Intensity *versus* angular position of the third-order reflection. Successive time frames are shifted upwards vertically, for easy comparison. 1, frame 1. In reality, frames 2–11 overlie each other. Dotted lines indicate the angular position of the peak intensity for the pre-transient time frame and for all subsequent time frames.

detector for higher-order reflections at wider diffraction angles.) Fig. 5B shows the corresponding angular distribution of intensity of the third-order reflection for all 11 time frames. Again, the intensity of the pre-transient pattern (marked 1) is lower than those for the 10 other patterns taken during the transient. There is an indication of changes in the overall orientation of collagen between pattern 1 and the subsequent patterns, as shown by a shift to higher angles in the subsequent patterns of the peak centred on 175° in pattern 1. However, no systematic difference was observed between the angular distribution of intensity for frames 2–11, indicating that there was no time-dependent reorientation during the time course of the transient. This result was typical of all X-ray diffraction results from stress-relaxation tests on both skin and perimysium; no reorientation during the stress-relaxation transient was seen in any experiment. For clarity, only stress-relaxation tests at high levels of pre-strain are shown here, because these showed the most obvious stress-relaxation behaviour and had strong X-ray patterns. However, the same lack of time-dependent reorientation was evident during stress-relaxation tests at low and medium pre-strains.

Fig. 6A shows the radial spacing and Fig. 6B the angular distribution of X-ray intensities from the 11 time frames taken during the creep experiment on rat skin depicted in Fig. 3C. The intensity of the third- and fifth-order diffraction maxima again increased between the pattern immediately before loading and the 10 patterns taken during the loading transient but, as Fig. 6A shows, there was no change in the radial position of the maxima, indicating that there was no change in the D-spacing. Changes in the relative intensity of the Bragg peaks would indicate changes in the axial molecular packing of the collagen molecules; as such changes are not apparent (especially for the first-, third- and fifth-order peaks), there is no evidence to suggest that the gap-overlap structure of molecular packing within the collagen fibres changes during these transients. The reorientation of collagen between pre-transient and during transient patterns is clearly evident from Fig. 6B, as represented by the shift in the peak centred on 167° in pattern 1 to approximately 175° in subsequent patterns. However, no angular shift between patterns for frames 2–11 can be seen, showing that no discernible reorientation took place during the creep transient. This result was typical of all creep experiments on both perimysium and skin at the light load levels used.

Discussion

Reorientation of collagen fibres due to finite extension of connective tissues is a well-documented and theoretically analysed phenomenon (Aspden, 1986) that gives rise to the non-linear load extension curve of both skin (Veronda and Westmann, 1970) and perimysium (Purslow, 1989). It is the time-dependent aspect of the properties of extensible connective tissues that requires explanation and is under study here. In both stress-relaxation and creep tests, the observation of differences in the intensity and angular position of diffraction maxima corresponding to the third and fifth orders of the meridional D-spacing along the length of collagen molecules

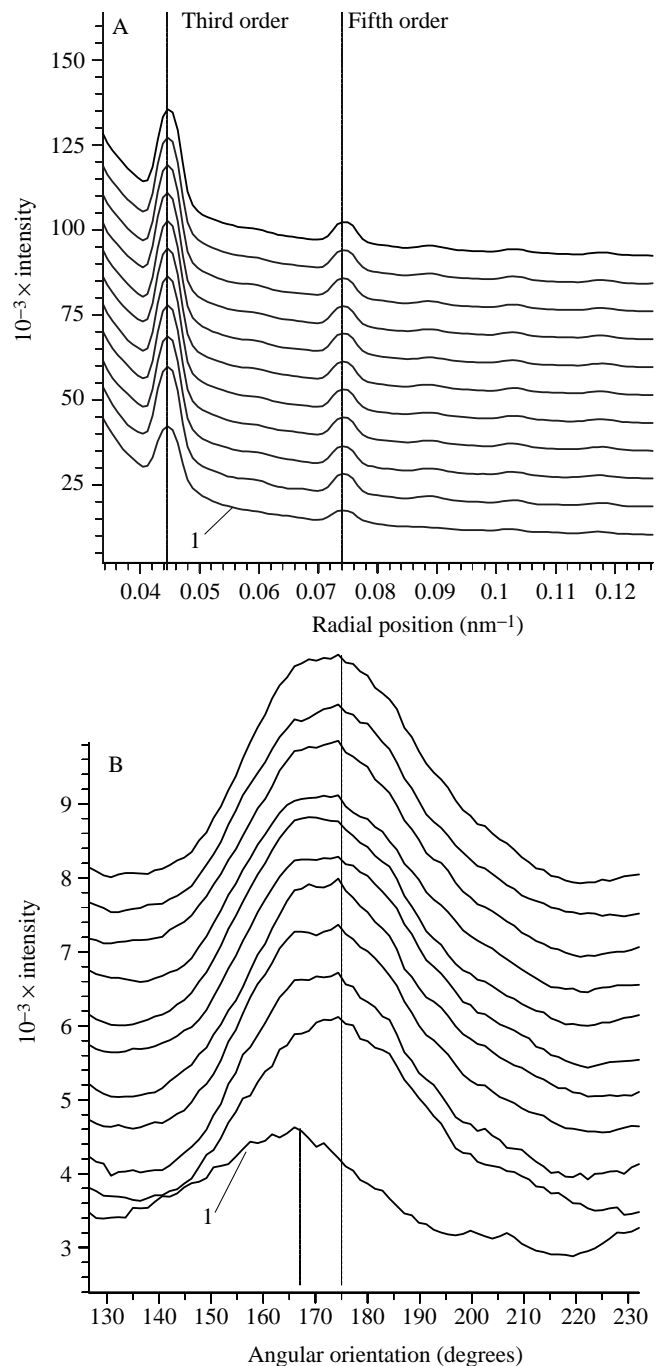


Fig. 6. Meridional spacing and angular distribution of intensity maxima during creep in rat skin. (A) Intensity *versus* radial position and (B) intensity *versus* angular position of the third-order reflection. As in Fig. 5, successive time frames are shifted vertically upwards. Dotted lines have the same interpretation as in Figs 5A,B.

before and after the application of a transient indicates the ability of X-ray diffraction to distinguish structural rearrangements of collagen networks within the tissues studied. That no obvious reorientation is observed during the time course of either a strong stress-relaxation or creep transient indicates that long-range reorientation of collagen fibres is not a principal structural event associated with the viscoelastic

behaviour of these tissues. A lack of temporal correlation between reorientation and stress-relaxation was observed over a range of strains, although strong stress-relaxation behaviour is only seen at high levels of pre-strain.

Significant stress-relaxation is seen (principally at medium to high pre-strain levels) in skin and perimysium, as shown in Fig. 3A,B. In stress-relaxation, the holding of the specimen at a fixed extension means that no macroscopic strain-induced reorientation of collagen should be expected during the test. Only internal rearrangement within tissue held between fixed clamps is possible. Internal rearrangement of collagen network morphology could be driven by the initial strain energy imparted to the specimen on stretching, which gradually diminishes as the stress relaxes. At rest length, the collagen fibres in perimysium are regularly crimped or wavy, and time-dependent reorganisation of the crimps could occur without any change in their overall orientation. The collagen fibres in skin are irregularly curved in resting tissue, but could also accommodate local changes in fibre geometry that would necessitate small translations of segments of the fibres with respect to the surrounding proteoglycan matrix. The curvilinearity of collagen fibres is most pronounced at rest length and diminishes as the tissue is extended. This is also observed in other connective tissues such as endomysium (Purslow and Trotter, 1994). In the simple crossed-ply arrangement of crimped collagen fibres in perimysium, the rate of change of crimp angle with extension of the tissue has been calculated (Purslow, 1989) and is maximal at rest length with a periodicity of approximately $50\mu\text{m}$. It diminishes rapidly at higher extensions, as the fibres are straightened out. Thus, if de-crimping of collagen is a possible mechanism underlying the viscoelastic behaviour of CTs, the greatest viscoelastic effect would be seen at rest length, with diminishing time-dependent behaviour at higher extensions.

In common with many biological materials (Fung, 1980), the

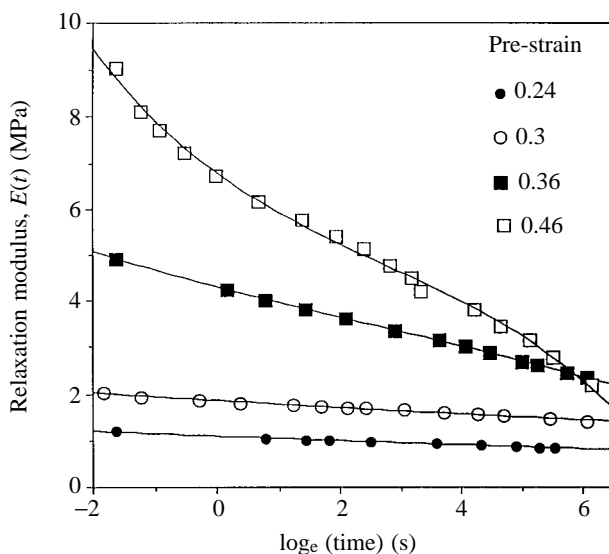


Fig. 7. Relaxation modulus $E(t)$ versus $\ln(\text{time})$ from stress-relaxation tests on a single specimen of perimysium at increasing levels of pre-strain. Relaxation is greatest from higher pre-strain levels.

present mechanical studies of perimysium show it to be non-linearly viscoelastic, i.e. the magnitude of the viscoelastic response depends on strain. However, the greatest relaxation in this tissue is seen at the highest extensions, when the collagen fibres would be expected to be straightened out. This is demonstrated in Fig. 7, which compares the stress relaxation behaviour of perimysium for a given step change in length, but starting from a variety of initial pre-extensions. The greatest relaxation behaviour is seen at large pre-extensions, when the collagen fibres are already fairly well-aligned to the stretching axis and are straightened. This observation argues that the molecular processes responsible for stress-relaxation do not involve straightening of the fibres. Because significant relaxation is seen when the collagen fibres are straightened and bearing significant load, it is reasonable to suppose that the relaxation processes may occur within the fibres themselves, or possibly at their surface connections to the matrix. These possibilities could be quite similar if the fibres are viewed as composite hierarchical structures of discontinuous supramolecular assemblies bound together by interfibrillar matrix (Cribb and Scott, 1995). Stress-relaxation within individual molecules of a fibrous protein has been demonstrated in the case of the cytoskeletal protein titin found in muscle (Tskhovrebova *et al.* 1997).

Mosler *et al.* (1985) did observe changes in the 67 nm D-period spacing in rat tail tendon and human digital flexor tendon under load. They note that, in these axially aligned assemblies of collagen fibres, if a constant displacement is applied (i.e. in a stress-relaxation experiment), an initial increase in D-spacing occurs, but this relaxes back to the original 67 nm value at a rate which is much faster than the rate of stress-relaxation. They also report a sustained increase in D-period of some 1.8% when tendon is held at a constant load (i.e. creep test conditions) near the breaking point of the tendon. They conclude that there are

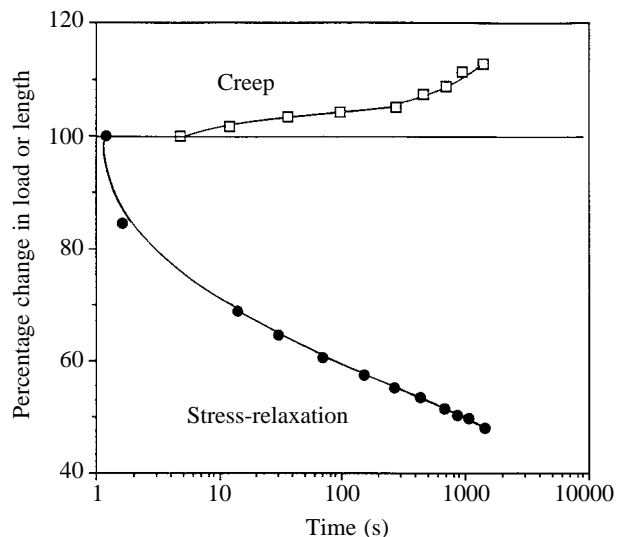


Fig. 8. Creep versus stress-relaxation in skin. The two curves are normalised to 100% at the beginning of the transient. Comparison of these normalised curves shows that the creep is not simply the inverse of stress-relaxation, but has a different time course. Each curve is the result of a test on a single specimen.

no continuous fibrils or subfibril units through the length of a fibre, but that force is transferred from overlapping units by some linkage (matrix) between them that allows the molecular aggregates of collagen to slide with respect to each other. Increases in the 67 nm spacing (64 nm in dry tissue) and the much smaller 0.29 nm spacing arising from the amino acid repeat distance in the helical structure of the collagen molecule have been reported in X-ray diffraction studies of dry collagen under load (Cowan *et al.* 1955). However, the plasticising effect of water is not present in such tests. The studies of Mosler *et al.* (1985) therefore examined the spacing changes in collagen in a more physiologically relevant state.

Creep and stress-relaxation represent two different kinds of mechanical event in a viscoelastic tissue. In creep, the continued extension of the material under constant load means that reorientation due to increasing overall strain in the specimen can occur, driven by the strain energy imparted to the specimen which increases with time. The two processes have very different time courses even in the same tissue, as demonstrated in Fig. 8; the proportional change of strain from the initial value in a creep test on rat skin is much less than the proportional amount of stress-relaxation over the same time course. From the forgoing, and from the observations of Mosler *et al.* (1985) on aligned collagen in tendons subject to high loads, we might have expected some change in both overall orientation and radial spacing of collagen in our experiments. However, the stresses applied to our tissues (0.01–0.05 MPa) were very much lower than those used by Mosler *et al.* (1985), which may explain why no D-spacing increases were observed. The comparatively small amount of length change seen in the creep experiments reported here may also explain why no overall reorientation of collagen was seen during the transient. However, even though low loads were used in the creep tests described here, they were sufficient to elicit a detectable time-dependent creep response in the tissue. More investigations are required at a higher range of applied load in order to determine whether the changes in D-spacing seen by Mosler *et al.* (1985) in their creep tests on tendon can also be induced in tissues composed of a disorientated network of collagen fibres.

In conclusion, large-scale reorientation of collagen is not seen during the time course of creep and stress-relaxation viscoelastic transients in skin and perimysium, two examples of extensible connective tissues. Reorientation of collagen fibres through a viscous matrix does not therefore seem to be the principal mechanism underlying the viscoelastic behaviour of these tissues. Three other possible mechanisms are (a) relaxation processes in the matrix surrounding the collagen fibres, (b) relaxations within the fibres themselves, or (c) time-dependent effects at the interface between fibre and matrix. The observation of most marked relaxation only at high stresses/high extensions when significant forces are borne by the collagen fibres indicates that the latter two explanations are more likely than the first, i.e. that the viscoelastic mechanism resides within the collagen fibres or at the interface between fibre and matrix.

We gratefully acknowledge the support of CLRC in granting beam-time on station 2.1 of the Synchrotron Radiation Source at Daresbury Laboratory and the help and advice of Sue Slawson, Liz Towns-Andrews and John Harries in its use.

References

- ASPDEN, R. M. (1986). Relation between structure and mechanical behaviour of fibre reinforced composite materials at large strains. *Proc. R. Soc. B* **212**, 299–304.
- BIGI, A., RIPAMONTI, A., ROVERI, N., JERONIMIDIS, G. AND PURSLOW, P. (1981). Collagen orientation by X-ray pole figures and mechanical properties of medial carotid wall. *J. Mater. Sci.* **16**, 2557–2562.
- COWAN, P. M., NORTH, A. C. T. AND RANDALL, J. T. (1955). X-ray diffraction studies of collagen fibres. In *Fibrous Proteins and Their Biological Significance* (ed. R. Brown and J. F. Danielli), pp. 115–126. Cambridge: Cambridge University Press.
- CRIBB, A. M. AND SCOTT, J. E. (1995). Tendon response to tensile stress: an ultrastructural investigation of collagen:proteoglycan interactions in stressed tendon. *J. Anat.* **187**, 423–428.
- DORRINGTON, K. L. (1980). The theory of viscoelasticity in biomaterials. In *The Mechanical Properties of Biological Materials* (ed. J. F. V. Vincent and J. D. Currey), pp. 289–314. Cambridge: Cambridge University Press.
- FUNG, Y. C. (1980). *Biomechanics*. Berlin: Springer-Verlag.
- GABELLA, G. (1987). The cross-ply arrangement of collagen fibres in the submucosa of the mammalian small intestine. *Cell Tissue Res.* **248**, 491–497.
- HALL, C. AND LEWIS, R. (1994). Recent developments in X-ray detectors for synchrotron-radiation experiments. *Nuclear Instr. Meth. Phys. Res.* **348**, 627–630.
- HAMMERSLEY, A. P. (1993). FIT2D: A scientific data analysis program. *ESRF Internal Report EXP/AH/93-02*.
- KLEIN, J. A. AND HUKINS, D. W. L. (1982). Collagen fiber orientation in the annulus fibrosus of intervertebral disk during bending and torsion measured by X-ray diffraction. *Biochim. biophys. Acta* **719**, 98–101.
- MOSLER, E., FOLKHARD, W., KNÖRZER, E., NEMETSCHKE-GANSLER, H. AND NEMETSCHKE, T. (1985). Stress-induced molecular rearrangement in tendon collagen. *J. molec. Biol.* **182**, 589–596.
- PURSLOW, P. P. (1989). Strain-induced reorientation of an intramuscular connective tissue network: implications for passive muscle elasticity. *J. Biomech.* **22**, 21–31.
- PURSLOW, P. P. AND TROTTER, J. A. (1994). The morphology and mechanical properties of endomysium in series-fibred muscles; variations with muscle length. *J. Muscle Res. Cell Motil.* **15**, 299–304.
- ROVERI, N., RIPAMONTI, A., PULGA, C., JERONIMIDIS, G., PURSLOW, P. P., VOLPIN, D. AND GOTTE, L. (1980). Mechanical behaviour of aortic tissue as a function of collagen orientation. *Makromol. Chem.* **181**, 1999–2007.
- ROWE, R. W. D. (1974). Collagen fibre arrangement in intramuscular connective tissue. *J. Food Technol.* **9**, 501–508.
- TSKHOVREBOVA, L., TRINICK, J., SLEEP, J. A. AND SIMMONS, R. M. (1997). Elasticity and unfolding of single molecules of the giant muscle protein titin. *Nature* **387**, 308–312.
- VERONDA, D. R. AND WESTMANN, R. A. (1970). Mechanical characterisation of skin – finite deformations. *J. Biomech.* **3**, 111–124.
- WAINWRIGHT, S. A., BIGGS, W. D., CURREY, J. D. AND GOSLINE, J. M. (1976). *Mechanical Design in Organisms*. London: Edward Arnold.